Available online at www.sciencedirect.com
ScienceDirect
Journal of Nuclear Materials 366 (2007) 37–51
journal of nuclear materials
www.elsevier.com/locate/jnucmat

A model for predicting coolant activity behaviour for fuel-failure monitoring analysis

B.J. Lewis [a,*], A. El-Jaby [a], J. Higgs [a], W.T. Thompson [a], F.C. Iglesias [b], R. Laidler [b], J. Armstrong [b], R. Stone [b], R. Oduntan [b]

[a] Department of Chemistry and Chemical Engineering, Royal Military College of Canada, Kingston, Ont., Canada K7K 7B4
[b] Bruce Power, 700 University Avenue, Toronto, Ont., Canada M5G 1X6

Received 9 August 2006; accepted 28 November 2006

Abstract

A mathematical treatment has been developed to predict the release of volatile fission products from operating defective nuclear fuel elements. The activity in both the fuel-to-clad gap and coolant as a function of time can be predicted during all reactor operations including steady operation as well as reactor shutdown, startup and bundle-shifting maneuvers. The model has been implemented as the STAR (Steady-state and Transient Activity Release) code based on a finite-element solution of the mass transport equations. The model parameters are derived from in-reactor experiments conducted with defective fuel elements containing natural and artificial failures at the Chalk River Laboratories. The STAR code has also been successfully validated against an analytical solution and benchmarked against several defect occurrences in a commercial reactor.

1. Introduction

With the occurrence of defective fuel, coolant can enter into the fuel-to-sheath gap and fission products (i.e., notably the volatile species of noble gas and iodine) will be released into the primary coolant [1–5]. With the entry of high-pressure coolant through the defect, the fuel may be oxidized that can potentially enhance the fission product release [6,7]. Iodine release can also occur on reactor shutdown when the temperature in the fuel-to-sheath gap drops below the saturation temperature, permitting liquid water to dissolve the soluble iodine species in the gap resulting in an 'iodine-spiking' phenomenon [8–11]. Iodine-rich water remaining in the gap on the subsequent startup can also be released as the size of the gap is reduced with fuel expansion [12].

Defective fuel elements can release fission products and fuel debris into the primary heat transport system (PHTS) [13], which will increase the circuit contamination and radiation exposure during maintenance. Operation in a defected condition can cause a reduced heat transfer in the fuel-to-sheath gap as well as oxidation of the fuel, which

* Corresponding author. Tel.: +1 613 541 6611; fax: +1 613 542 9489.
E-mail address: lewis-b@rmc.ca (B.J. Lewis).

0022-3115/$ - see front matter © 2007 Elsevier B.V. All rights reserved.
doi:10.1016/j.jnucmat.2006.11.015

may degrade the thermal performance of the element. In particular, fuel oxidation can result in a decrease in the thermal conductivity of the fuel and a reduced melting temperature for the hyperstoichiometric urania [14–17]. It is therefore desirable to discharge defective fuel bundles as soon as possible. Hence, a better understanding of defective fuel behaviour is required in order to develop an improved methodology for fuel-failure monitoring and coolant activity prediction.

Previous models have been developed for fuel-failure monitoring in both light water reactors (LWR) and the CANDU reactor based on a steady-state coolant activity analysis [3,18–20]. These models employ a 'Booth-diffusion' type model [21–23] for release from the fuel matrix into the fuel-to-sheath gap and a first-order kinetic model to account for the transport, holdup and release of the short-lived fission products from the gap into the primary coolant. In such analysis, it is necessary to use an 'empirical diffusion coefficient' to account for the fission product diffusion in the fuel [21] and a 'gap escape-rate coefficient' for release from the gap [3,18–20]. Unfortunately, these parameters are not constant in time as they are influenced by the defect condition (which can deteriorate with time as a result of sheath hydriding/secondary deterioration) [4]. As the element deteriorates and the size of defect increases there is less holdup of the short-lived fission products in the gap (and hence a changing gap escape-rate coefficient). The fission product diffusivity is also enhanced with continued fuel oxidation [24]. Moreover, complex thermal hydraulic effects will result in the gap on shutdown as the pellet contracts and water enters into the fuel element on shutdown [12]. During reactor shutdown, the gap escape-rate coefficient is further enhanced via ionic (Nernst) diffusion of iodine in liquid water in comparison to simple diffusional transport that occurs at operating powers with the presence of steam in the gap as described by Chapman–Enskog kinetic theory [8]. On the subsequent reactor startup, the expansion of the fuel will force water out of the fuel-to-sheath gap resulting in a convective release [12]. These complicated effects can be incorporated into the model via a (variable) gap escape-rate coefficient. Hence, the model parameters characterizing the fission product transport must be fit to the coolant activity data. In fact, for the previous steady-state analysis tools [3,18–20], the model is fit to coolant activity data and the fitted parameters are compared to experimental values where the defect state was well characterized in order to ascertain the fuel-defect condition. However, with this steady-state type of analysis, it is possible to trade off the gap escape-rate coefficient (which characterizes the defect size) against the element linear power (which affects the empirical diffusion coefficient) in the model fitting which will lead to an uncertainty in the given analysis. A number of isotopes of both noble gases and radioiodines are therefore needed for a more accurate analysis to minimize this problem; however, coolant activity data typically supplied by the stations are generally limited to just a few isotopes, e.g., ^{131}I, ^{133}Xe, ^{135}Xe and ^{88}Kr which again results in greater uncertainty in the model application and prediction. Moreover, the application of the previous models specifically requires that steady-state (equilibrium) conditions have been met. However, a preponderance of coolant activity data involves a time dependence associated with reactor shutdown/startup and bundle-shifting operations, which particularly arise in the CANDU reactor with its ability for on-power refueling. Other theoretical treatments have only focused on the shutdown event in order to account for iodine-spiking phenomena (which again requires a fitting of the model to available coolant activity data) [8,10,11]. Hence, a more general treatment is needed which can make use of all available data and is applicable for all operating reactor conditions. Thus, the approach presented in this work synthesizes all previous theoretical treatments with the development of a general time-dependent model using a finite-element numerical approach. This model is able to predict the activity behaviour in the fuel grain, fuel-to-sheath gap and primary coolant, respecting the overall mass balance under all reactor conditions.

In the current approach, the same gap escape-rate coefficient must be used for all isotopes of the same chemical species (for either noble gas or iodine). In addition, the same diffusion coefficient is used for all species (and their precursors). In addition, this mathematical formulation must be able to follow the complete transient behaviour of the coolant activity concentration for all isotopes observed (with a given decay constant). The model must also specifically take into consideration the changing fission product concentration distribution within the fuel grain for all isotopes of interest incorporating effects of radioactive decay and neutron transmutation. As such, as detailed in Section 2, this more general treatment requires a complete and

coupled numerical solution of a partial differential equation for diffusion of the fission products in the fuel matrix as well as two ordinary differential equations for transport in the gap and primary coolant that respects the mass balance for a time-varying fission product generation and coolant purification flow history. This type of analysis provides for a more accurate analysis than the steady-state approach since a unique solution is required for the model fitting parameters in order to reproduce the time-dependent coolant activity behaviour.

2. Model development

A fission product diffusion model coupled with a mass balance in the gap and coolant can be used to predict the coolant activity behaviour for both steady-state and transient reactor operation. The model can be developed for variable reactor power and coolant purification histories. In this way, the model can be matched to coolant activity trends and then used in a prognostic manner to predict the coolant activity behaviour as a function of reactor power and the coolant purification history.

The radial diffusion equation for the concentration distribution $C(r,t)$ at time t, based on a 'Booth-diffusion' model for an idealized fuel grain sphere of radius a, can be written as [21]

$$\frac{\partial C(r,t)}{\partial t} = \frac{D(t)}{r^2}\frac{\partial}{\partial r}\left(r^2\frac{\partial C(r,t)}{\partial r}\right) - \lambda C(r,t) + \frac{F_f(t)y}{V}, \tag{1}$$

where λ is the radioactive decay constant (s^{-1}), D is the diffusion coefficient for a given fission product species in the fuel matrix ($m^2\,s^{-1}$), F_f is the fission rate in the fuel (fission s^{-1}), y is the cumulative fission yield (atom fission^{-1}) and V is the fuel volume for the defective element. Defining the dimensionless variable, $\eta = r/a$, and multiplying through by V, Eq. (1) becomes

$$\frac{\partial u(\eta,t)}{\partial t} = \frac{D'(t)}{\eta^2}\frac{\partial}{\partial \eta}\left(\eta^2\frac{\partial u(\eta,t)}{\partial \eta}\right) - \lambda u(\eta,t) + F_f(t)y, \tag{2}$$

where $u = CV$ and $D' = D/a^2$. The initial and boundary conditions are given as

$$u(\eta,0) = 0, \quad 0 < \eta < 1, \quad t = 0, \tag{3a}$$

$$\frac{\partial u}{\partial \eta} = 0, \quad \eta = 0, \quad t > 0, \tag{3b}$$

$$u(1,t) = 0, \quad \eta = 1, \quad t > 0. \tag{3c}$$

The diffusional release to-birth rate ratio for the defective element is

$$\left(\frac{R}{B}\right)_{dif} = \frac{4\pi a^2}{F_f y(4\pi a^3/3)}\left(-D\left.\frac{\partial CV}{\partial r}\right|_{r=a}\right) = -\frac{3D'}{F_f y}\left.\frac{\partial u}{\partial \eta}\right|_{\eta=1}. \tag{4}$$

Equivalently, the release rate R_{dif} (atom s^{-1}) from the defective fuel element is

$$R_{dif} = -3D'\left.\frac{\partial u}{\partial \eta}\right|_{\eta=1}. \tag{5}$$

Thus, the time-dependent diffusion equation in Eq. (2) can be solved by numerical methods subject to the conditions in Eqs. (3a)–(3c). The derivative of this solution (at $\eta = 1$) is subsequently used in Eq. (5). Eq. (5) is the source release rate from the fuel matrix into the fuel-to-clad gap for the defective element and can be used in the mass balance for the gap:

$$\frac{dN_g(t)}{dt} = R_{dif}(t) - (\lambda + v(t))N_g(t). \tag{6a}$$

Here, assuming a first-order rate process for fission product release from the gap, the escape rate/leaching rate coefficient v (s^{-1}) can be considered as a function of time. Also, during reactor shutdown, an enhanced leaching rate constant is used for v so that the model can also reproduce 'iodine-spiking' phenomena. The parameter v can also be adjusted to reproduce convective release during other transient reactor operations. The initial condition for Eq. (6a) is

$$N_g(t) = 0, \quad t = 0. \tag{6b}$$

The mass balance in the coolant is similarly given by

$$\frac{dN_c(t)}{dt} = v(t)N_g(t) - (\lambda + \beta_p(t))N_c(t) \tag{7a}$$

with a time-dependent coolant purification rate constant $\beta_p(t)$. This equation is subject to the initial condition:

$$N_c(t) = 0, \quad t = 0. \tag{7b}$$

Eq. (7a) neglects for any release of fission products from fuel debris as a result of fuel loss from the defective element(s). In this latter case, the fission product release process is due to direct recoil from small particles of fuel debris (i.e., individual fuel grains lost by grain boundary oxidation and coolant erosion under the defect site), which have deposited on the in-core piping surfaces of the primary heat transport system

[2,13,25,26]. As shown in Ref. [2], this source of release is typically negligible compared to that released from the defective element, especially for the longer-lived isotopes (e.g., ^{131}I and ^{133}Xe).

The solution of the coupled Eqs. (2), (3), (5)–(7) provides a prediction of both the gap and coolant activity as a function of time for a variable fuel element linear rating/reactor power and coolant purification history. One can further follow the degradation of a fuel element with a changing value of the escape rate/leaching rate coefficient, where this parameter can be used as a tuning parameter to match the observed coolant activity data (with a knowledge and input of the operational data for the purification flow and reactor power history).

2.1. Precursor effects for I-132 and Xe-135

For isotopes that have relatively long-lived precursors, precursor effects must be considered [1,20]. Thus, the model can be further generalized for the isotopes of ^{132}I and ^{135}Xe to account for precursor diffusion as well as neutron transmutation effects. The latter effect is only important for the isotope ^{135}Xe. For parent (p)–daughter (d) diffusion, using the given variable transformation, gives

$$\begin{aligned}\frac{\partial u_{\mathrm{p}}}{\partial t} &= \frac{D'_{\mathrm{p}}(t)}{\eta^2}\frac{\partial}{\partial \eta}\left(\eta^2\frac{\partial u_{\mathrm{p}}}{\partial \eta}\right) - \lambda_{\mathrm{p}}u_{\mathrm{p}} + F_{\mathrm{f}}(t)y_{\mathrm{p}}^{\mathrm{c}},\\ \frac{\partial u_{\mathrm{d}}}{\partial t} &= \frac{D'_{\mathrm{d}}(t)}{\eta^2}\frac{\partial}{\partial \eta}\left(\eta^2\frac{\partial u_{\mathrm{d}}}{\partial \eta}\right) - (\lambda_{\mathrm{d}} + \sigma_{\mathrm{a}}\phi_{\mathrm{T}}(t))u_{\mathrm{d}}\\ &\quad + \lambda_{\mathrm{p}}u_{\mathrm{p}} + F_{\mathrm{f}}(t)y_{\mathrm{d}}^{\mathrm{d}},\end{aligned} \tag{8}$$

where the decay of the parent isotope provides for a source of the daughter isotope. Here σ_{a} is the neutron microscopic absorption cross section for ^{135}Xe, ϕ_{T} is the thermal neutron flux, $y_{\mathrm{p}}^{\mathrm{c}}$ is the cumulative fission yield for the parent and $y_{\mathrm{p}}^{\mathrm{d}}$ the direct yield for the daughter. Both the parent and daughter are subject to the initial and boundary conditions given in Eqs. (3a)–(3c). The diffusional source release rate into the fuel-to-sheath gap can again be evaluated from a Fick's law of diffusion [21]:

$$R_{\mathrm{dif,p}} = -3D'_{\mathrm{p}}\left.\frac{\partial u_{\mathrm{p}}}{\partial \eta}\right|_{\eta=1}, \tag{9a}$$

$$R_{\mathrm{dif,d}} = -3D'_{\mathrm{d}}\left.\frac{\partial u_{\mathrm{d}}}{\partial \eta}\right|_{\eta=1}. \tag{9b}$$

Similarly, the coupled mass balance equations for the gap and coolant for these isotopes are given respectively by

$$\frac{\mathrm{d}N_{\mathrm{g,p}}}{\mathrm{d}t} = R_{\mathrm{dif,p}}(t) - (\lambda_{\mathrm{p}} + v_{\mathrm{p}}(t))N_{\mathrm{g,p}}, \tag{10a}$$

$$\frac{\mathrm{d}N_{\mathrm{g,d}}}{\mathrm{d}t} = R_{\mathrm{dif,d}}(t) + \lambda_{\mathrm{p}}N_{\mathrm{g,p}} - (\lambda_{\mathrm{d}} + \sigma_{\mathrm{a}}\phi_{\mathrm{T}} + v_{\mathrm{d}}(t))N_{\mathrm{g,d}} \tag{10b}$$

and

$$\frac{\mathrm{d}N_{\mathrm{c,p}}}{\mathrm{d}t} = v_{\mathrm{p}}(t)N_{\mathrm{g,p}} - (\lambda_{\mathrm{p}} + \beta_{\mathrm{p,p}}(t))N_{\mathrm{c,p}}, \tag{11a}$$

$$\frac{\mathrm{d}N_{\mathrm{c,d}}}{\mathrm{d}t} = v_{\mathrm{d}}(t)N_{\mathrm{g,d}} + \lambda_{\mathrm{p}}N_{\mathrm{c,p}} - (\lambda_{\mathrm{d}} + \beta_{\mathrm{p,d}}(t) + f_{\mathrm{c}}\sigma_{\mathrm{a}}\phi_{\mathrm{T}})N_{\mathrm{c,d}}, \tag{11b}$$

where f_{c} is the fraction of the PHTS mass which is in-core. The initial conditions for both the parent and daughter isotopes are again given by Eqs. (6b) and (7b).

The system of partial differential equations (PDEs) has been solved as the Steady-state and Transient Activity Release (STAR) code using the commercial FEMLAB software package (Version 3.1) that employs a finite-element technique [27]. The STAR code is very versatile and can be restarted from the last solution of a previous simulation. In addition, the variables of interest can be continually changed to account for the time-dependence of the escape-rate coefficient, purification constant or power history.

3. Star code validation

The numerical implementation of the code can be tested against an analytical solution. The model can be further evaluated against in-reactor experiments conducted with well-characterized fuel failures in the X-2 defect loop at the Chalk River Laboratories (CRL) [4]. This evaluation permits a good opportunity to test the model and to specifically evaluate the model parameters. Finally, the model can be tested against actual defect experience in the commercial power reactor where the number of failures, and element power rating and coolant purification histories are known.

3.1. Comparison of numerical model against analytical solutions

The numerical solution of the coupled mass transport equations can be compared to an analytical solution for the coolant activity A_{c} ($=\lambda N_{\mathrm{c}}$) as derived in Ref. [28] for the long-lived isotope ^{129}I ($\lambda = 1.40\times10^{-15}$ s^{-1} and $y = 0.00744$ atom/fission):

$$A_c(t) = \mu F_f y\left\{\frac{1-e^{-\phi\tau}}{\phi} + \left(\frac{e^{-\psi\tau}-e^{-\phi\tau}}{(\psi-\phi)}\right)\frac{3}{\psi}[1-\sqrt{\psi}\cot\sqrt{\psi}] + 6\psi\sum_{n=1}^{\infty}\left(\frac{e^{-\phi\tau}-e^{-n^2\pi^2\tau}}{n^2\pi^2(n^2\pi^2-\psi)(n^2\pi^2-\phi)}\right)\right\}, \quad (12)$$

where $\mu = \lambda/D'$, $\tau = D't$, $\psi = v/D'$ and $\phi = \beta_p/D'$. The analytical solution in Eq. (12) implicitly neglects a source of release from possible fuel debris that could exist on the primary heat transport piping (i.e., consistent with the model development in Section 2) [28]. This result further assumes that there is no initial concentration profile in the fuel grain and no initial fission product inventory in the gap or coolant. The analytical result in Eq. (12) is also only applicable for constant coefficients of D', F_f, v and β_p. This analysis assumes a fission rate of $F_f = 5.96\times10^{14}$ fission s^{-1}, gap escape-rate coefficient of $v = 1.4\times10^{-6}\ s^{-1}$, coolant purification rate constant of $\beta_p = 7.05\times10^{-5}\ s^{-1}$, empirical diffusion coefficient of $D' = 4.57\times10^{-10}\ s^{-1}$ and PHTS mass of 244 Mg. For the analytical solution, 200 terms were considered in the infinite series. A comparison of this analytical relation with STAR for the coolant activity of ^{129}I is shown in Fig. 1. Excellent agreement is observed indicating a proper numerical implementation of the STAR code.

3.2. Model parameter evaluation based on X-2 defect experiments

An experimental program with defective CANDU-type fuel elements was carried out at the CRL [4]. Failed elements with various degrees of sheath damage were irradiated in separate tests in the X-2 experimental loop of the National Research Experimental (NRX) reactor. A brief summary of the fuel operating parameters for the experiments considered in the current analysis is detailed in Table 1. The experiments involved the irradiation of fuel elements that were either artificially or naturally defected. An element was artificially defected prior to irradiation with machined slits in the fuel sheathing. Other elements were characteristic of hydride failures found in power plants, which resulted from small manufacturing flaws.

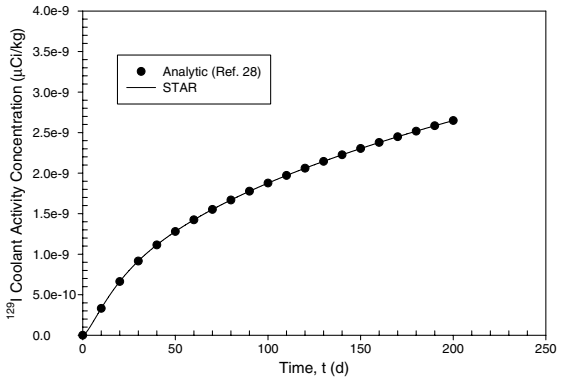

Fig. 1. Comparison of the analytic versus numerical solution for prediction of the coolant activity concentration of ^{129}I.

The X-2 defect experiments, which cover various operating conditions and different types of fuel failures, can provide data for validation of the model and an estimation of the model parameters. The multi-slit element A3N in experiment FFO-103 represents a 'worst-case' defect irradiated at a relatively high power of 48 kW/m where there is essentially no sheathing barrier so that fuel oxidation is maximized. Element A7A is a typical hydride failure that was previously irradiated in FFO-102-1 and FFO-102-3 and subsequently power-cycled in experiments FFO-110 and FFO-109 (Phase II) at low (14–26 kW/m) and intermediate (22–38 kW/m) linear powers. Finally, element A7E, which was irradiated in experiment FFO-102-1 and then reirradiated at a very high linear power of ~67 kW/m in FFO-102-2 (which is beyond normal commercial operating conditions), represents a severe hydride failure. Thus, these experiments cover a very broad range of operating powers and states of element deterioration.

The input conditions for the model were based on operational data [29–32]. The fission yields and decay constant were taken from Ref. [3]. For ^{135}Xe, a neutron absorption rate of $\sigma_a\phi_T = 7.862\times10^{-5}(P/51)\ s^{-1}$ was derived from a Wescott analysis of the X-2 loop experiments (i.e., as normalized to a linear power of $P = 51$ kW/m).

The gap escape-rate coefficients in the current model application were fixed and taken from a previous steady-state analysis of the X-2 experiments in [3] (see Table 2). However, these coefficients were increased by a factor of ~100 during the reactor startup period to account for enhanced (convective) release as the fuel-to-clad gap is reduced with fuel-pellet expansion [12]. For the multi-slit element, A3N, this effect was ignored since the gap inventory is expected to be much less due to the presence of many defects. On reactor shutdown, in order to model the 'iodine-spiking' phenomena, an enhanced gap escape-rate coefficient of $2\times10^{-5}\ s^{-1}$ (i.e., as suggested in [8]) was used for all analysis. This leaching rate coefficient accounted for enhanced

Table 1
Summary of experiments with single defective fuel elements at CRL

Experiment (element)	Test (defect) description	Defect size (mm^2)		Linear power (kW/m)	Burnup (MW h/kg U)		Defect residence time (effective full power days)	Fuel loss (g)
		Initial	Final		Initial	Final		
A. Artificially-defected fuel								
FFO-103 (A3N)	23 through-wall slits in a helical pattern along sheath (each slit 36 mm × 0.3 mm)	272	1490[a]	48	0	18	15	~65
B. Naturally-defected fuel								
FFO-102-1 (A7A)	Irradiation of elements with porosity in end caps	[b]	–	16	0	68	153	N/A
(A7E)		[b]	–	64	0	37	24	N/A
FFO-102-3 (A7A)	Reirradiation of element with incipient hydriding at low power	[b]	–	23	68	130	263	N/A
FFO-102-2 (A7E)	Reirradiation of element with through-wall hydriding at high power (cracked hydride blisters at one end of element)	11	300[b]	67	37	67	19	3.5
FFO-110 (A7A)	Power cycling of an element with	~0.5	–	14–26	130	140	281	N/A
FFO-109 (Phase 2) (A7A)	through-wall hydriding	–	~0.5	22–38	140	155	300	<0.1

N/A: not available (no metallography performed at this stage of irradiation).
[a] Slits enlarged during irradiation due to fuel expansion (defect size estimated from post-irradiation examination).
[b] Primary defect size for A7A (0.4 μm) and A7E (1.4 μm).

Table 2
Evaluation of model parameters

Experiment	O/U ratio	Linear power[a] (kW/m)	Model parameter							
			Empirical diffusion coefficient, D' (s^{-1})				Escape-rate coefficient, v (s^{-1})			
			Steady-state		Current[b]	ξ_{ox}	Steady-state		Current	
			I	NG			I	NG	I	NG
FFO-103	2.28	51.0	5.01×10^{-9}	2.14×10^{-9}	3.01×10^{-8}	26704	1.8×10^{-4}	2.3×10^{-4}	1.8×10^{-4}	2.3×10^{-4}
FFO-110	–	26.0	6.55×10^{-12}	6.38×10^{-12}	6.55×10^{-12}	114.0	–	–	6.8×10^{-8}	9.3×10^{-7}
FFO-109-2		33.0	6.86×10^{-11}	5.00×10^{-11}	1.10×10^{-10}	1077	6.8×10^{-8}	4.9×10^{-5}	6.8×10^{-8}	4.9×10^{-5}
FFO-102-2[c]	~2.14	66.6	4.46×10^{-10}	2.56×10^{-9}	3.80×10^{-9}	143.1	2.5×10^{-6}	8.4×10^{-6}	2.5×10^{-6}	8.4×10^{-6}

[a] Linear power at which steady-state diffusion coefficient was measured or maximum linear power.
[b] Evaluated with Eq. (13).
[c] The escape-rate coefficients were reduced by a factor of 3 (iodine) and increased by a factor of 1.5 (noble gas) during part of the irradiation history from the steady-state values proposed in [3].

ionic diffusion/natural convective transport with the presence of liquid water in the gap due to Nernst diffusion [8]. However, no release of noble gases is assumed to occur in the vertical elements with the presence of liquid water in the gap during the shutdown period. In accordance with the observations in Ref. [33], ^{132}Te is only assumed to be washed out of the gap on reactor shutdown with the same enhanced gap escape-rate coefficient (i.e., leaching rate coefficient) as assumed for iodine. The same gap escape rate coefficient is used for all isotopes of a given chemical species.

The empirical diffusion coefficients were fixed for a given experimental simulation. The same diffusion coefficient was used for all chemical species (i.e., iodine, noble gas and tellurium). This parameter accounts for the effect of intergranular (solid-state) diffusion, intra and intergranular bubble coalescence, grain-boundary interlinkage and grain-boundary sweeping. The value of the empirical diffusion for each experiment is comparable to that obtained in the previous steady-state analysis of Ref. [3]. A slight discrepancy arises since the latter analysis only pertains to a small sampling period whereas the current

analysis requires an average value over the whole irradiation period since the diffusion coefficient changes with increased fuel oxidation [24]. In particular, as shown in [17], the solid fuel will continually oxidize with time in a defective element.

The empirical diffusion coefficient as used in the model for oxidized fuel, D' (s^{-1}), was derived from a previous correlation as a function of the linear fuel element power P (kW/m) based on sweep gas experiments with unoxidized fuel (see Fig. 6 in Ref. [3]) [34]. This relation was multiplied by a simple enhancement factor (ξ_{ox}) to account for fuel oxidation effects (see Table 2 and Fig. 2(a)):

$$D'(P) = (\xi_{ox}) \exp\{a_0 + a_1 P + a_2 P^2\}, \quad (13)$$

where $a_0 = -30.856311$, $a_1 = -0.039332$ and $a_2 = 2.056960 \times 10^{-3}$. The effect of fuel cracking on reactor shutdown/startup, however, has not been modeled in the current simulations since this effect is expected to be of less importance [12,35].

As shown in Table 2 and Fig. 2(a), the diffusion coefficient for FFO-103 is specifically enhanced with a higher oxygen-to-uranium (O/U) ratio. A comparison of the (steady-state) empirical diffusion coefficients in Ref. [3] with the current fitted values is also shown in Fig. 2(b) and listed in Table 2. The empirical diffusion coefficient for experiment FFO-109-2 is in fact 'representative' of that for typical commercial power reactor experience where

$$D'(P) = 4.28 \times 10^{-11} \exp\{-0.03933 \cdot P + 0.00205696 \cdot P^2\}. \quad (14)$$

The range of the empirical diffusion coefficients seen in Fig. 2(a) is consistent with that seen for intact versus defective fuel rods in German pressurized water reactors (PWR) and boiling water reactors (BWR) in Fig. 3, where enhancement factors of ~300–1000 are typically seen for oxidized fuel that is in good agreement with the value of ξ_{ox} in Table 2 [36].

The fission product diffusion coefficient ($m^2\,s^{-1}$) in hyperstoichiometric fuel physically depends on intrinsic diffusion at high temperature, irradiation-enhanced vacancy production at intermediate temperature (i.e., the uranium vacancy concentration which is a function of the deviation from stoichiometry x in UO_{2+x}) and irradiation-enhanced (athermal) diffusion at low temperature [14]:

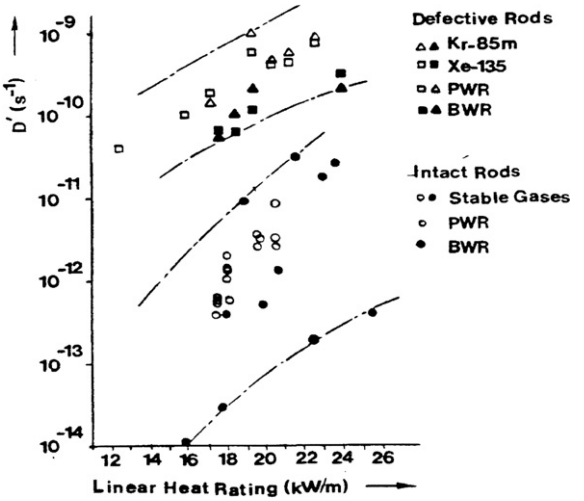

Fig. 3. Correlation of empirical diffusion coefficient versus linear heat rating for intact and defective German BWR and PWR fuel rods. Taken from Ref. [36].

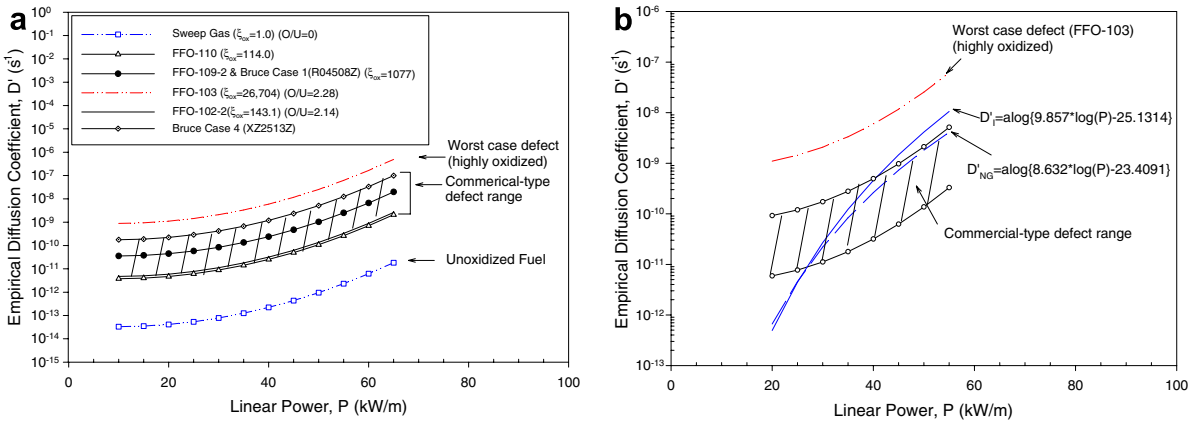

Fig. 2. Empirical diffusion coefficients as a function of the fuel element linear power for: (a) unoxidized and oxidized fuel in the current analysis; (b) comparison between the previous steady-state analysis and current work.

$$D(x,T) = 7.6\times10^{-10}\exp\left\{\frac{-35\,230}{T}\right\} + \left[\sqrt{2\dot{F}}\times10^{-25}\exp\left\{\frac{-13\,890}{T}\right\} + x^2 2.22\times10^{-8}\exp\left\{\frac{-20\,230}{T}\right\}\right] + 2\times10^{-40}\dot{F} \quad (15)$$

in which $\dot{F}$ is the fission rate density (fission m^{-3} s^{-1}) and T is the temperature (K). An empirical diffusivity for defective fuel can be alternatively obtained by scaling the diffusivity for unoxidized fuel (i.e., the sweep gas diffusivity) with a correction factor H such that [14]

$$D' = HD'_{\text{sweep}}, \quad (16)$$

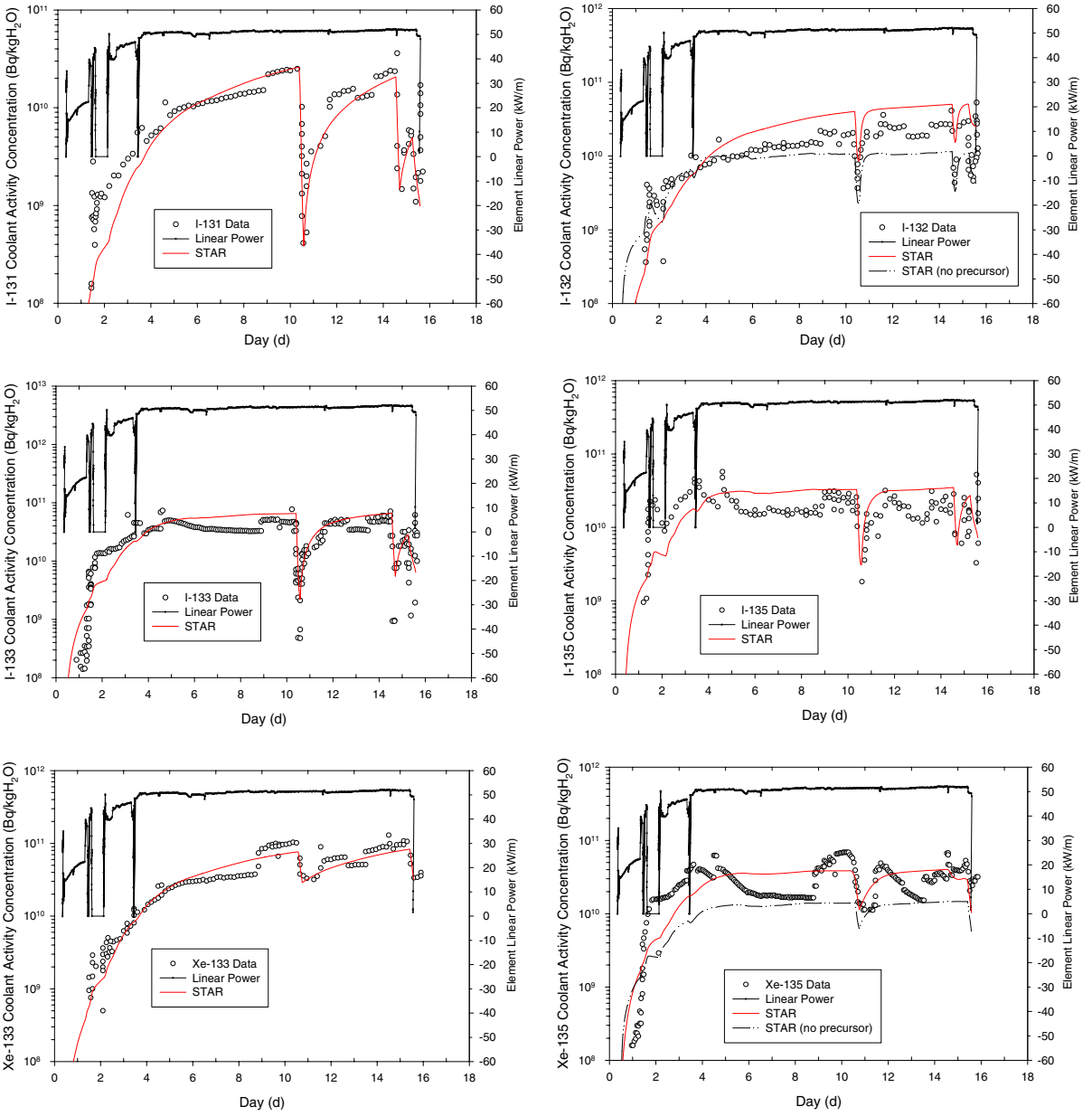

Fig. 4. Comparison between the measured and predicted coolant activity concentration history for iodine and noble gas species for experiment FFO-103.

where

$$H = \left\langle \frac{D(x,T)}{D(0,T)} \right\rangle_{\text{pellet}}. \quad (17)$$

Here the diffusion coefficient D is evaluated from Eq. (15) and H is obtained by averaging the oxidized-to-non-oxidized diffusion coefficient ratio for a given temperature and fuel stoichiometry deviation profile in the fuel pellet volume. Interestingly, over a linear power range of 20–60 kW m^{-1}, H is evaluated in Ref. [14] between 300 and 2300, which is also consistent with Fig. 3 and the value of ξ_{ox} in Table 2.

A comparison of the predicted and measured trends for the coolant activity concentration for the various experiments for several selected isotopes of iodine and noble gas is shown in Figs. 4–7. There is generally a good agreement between the model results and experimental data for all isotopes. As demonstrated in Figs. 4–7, precursor effects must be considered for the coolant activity concentration prediction of ^{132}I and ^{135}Xe.

3.3. Commercial reactor application

Representative fitting parameters for the fission product release model have been evaluated by benchmarking the model against coolant activity data derived from well-characterized failures in the X-2 defect program (Section 3.2). The model can now be applied for coolant activity analysis in the commercial reactor for several defective fuel cases.

A systematic assessment of the PHTS radionuclide activity in the commercial units was carried out [37,38]. Two representative cases were selected from this survey for analysis with STAR. These two specific cases were chosen since a single failure was known to be present in the core at the given time. The irradiation histories of the defect elements, as well as the purification operations, were determined from the historical data. The defective element linear powers were calculated from bundle power histories with the SORO code. Radionuclide activities of ^{131}I and ^{133}Xe were monitored in the commercial reactor. These activities were assessed with grab sample monitoring from the Chemistry

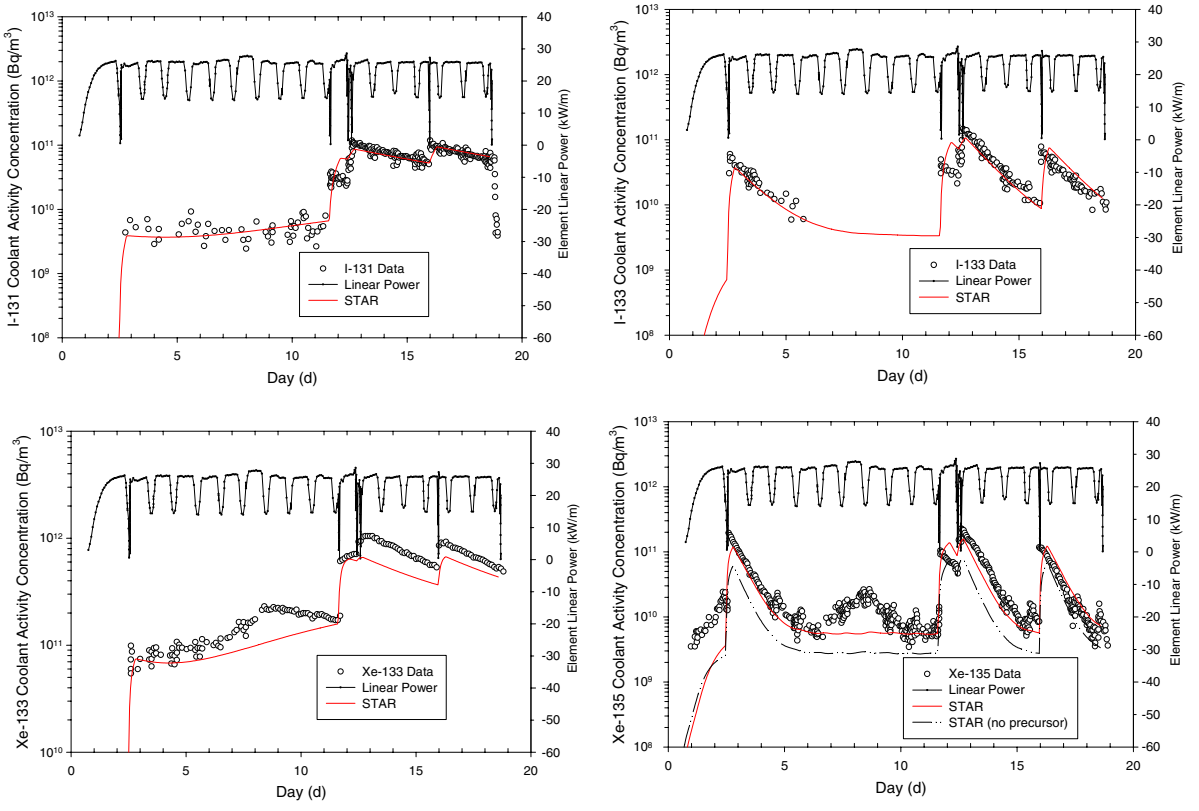

Fig. 5. Comparison between the measured and predicted coolant activity concentration history for iodine and noble gas species for experiment FFO-110.

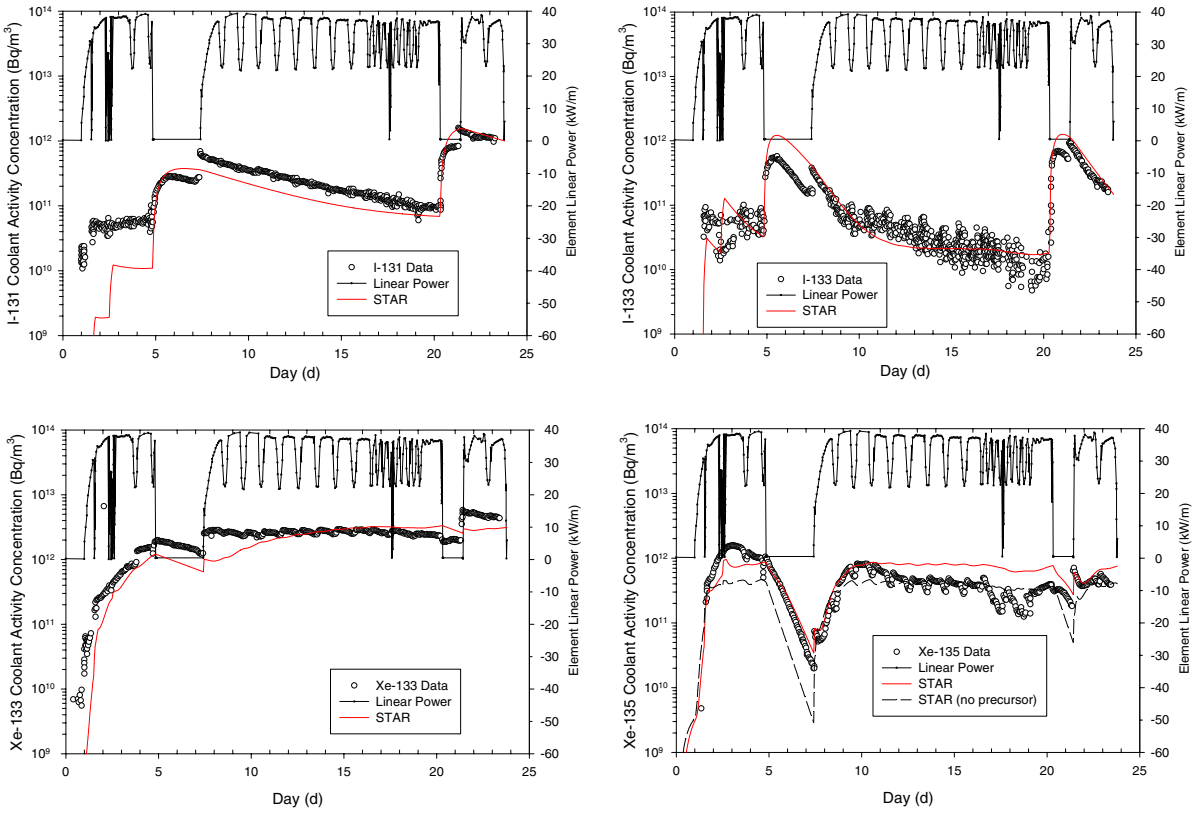

Fig. 6. Comparison between the measured and predicted coolant activity concentration history for iodine and noble gas species for experiment FFO-109-2.

Environmental Management (CEM) Database and with on-line gaseous fission product (GFP) monitoring from the Plant Information (PI) Database. Only activity levels greater than a preset threshold limit of 1 Ci were stored in the PI database whereas lower activities were available in the CEM database. Finally, the Fuels Inspection Database (FID) provided a documentation of the post-irradiation examination for these elements to enable a characterization of the defect sizes. These two cases as detailed in Table 3 can therefore be used to benchmark the STAR code for commercial operation with defective fuel.

The actual element linear powers and purification flows for these cases are shown in Figs. 8 and 9. These parameters (as input into STAR) are also shown along with the model input of the gap escape-rate coefficients. The gap escape-rate coefficients were fitted to reproduce the coolant activity concentrations. These fitted parameters are consistent with those values obtained for the X-2 experiments in Table 2. The empirical diffusion coefficients are also similar to those for the X-2 experiments in Fig. 2(a). The analysis for Case 1 uses Eq. (14), whereas Case 4 employs a coefficient that is five times greater. The same diffusion coefficient was used for both iodine and noble gas. A slightly larger coefficient had to be used for the Case 4 element since the defect was very large with a separated end cap leading, presumably, to greater fuel oxidation. For instance, the rare gas diffusion coefficient in hyperstoichiometric UO_{2+x} is seen to increase through the vacancy-enhanced component as the square of the stoichiometry deviation in Eq. (15) [14]. However, this coefficient was still lower than that observed for the 'worst-case' defect in experiment FFO-103.

The same diffusion coefficient as for experiment FFO-109-2 was employed for the Case 1 element since it had a small hydride blister. Prior to failure of the elements, an unoxidized diffusion coefficient (i.e., as determined from the sweep gas experiments in Fig. 2(a) with Eq. (13) for $\xi_{ox} = 1$) was employed in the simulation.

Excellent agreement is seen in the comparison of the measured coolant activity concentrations (from

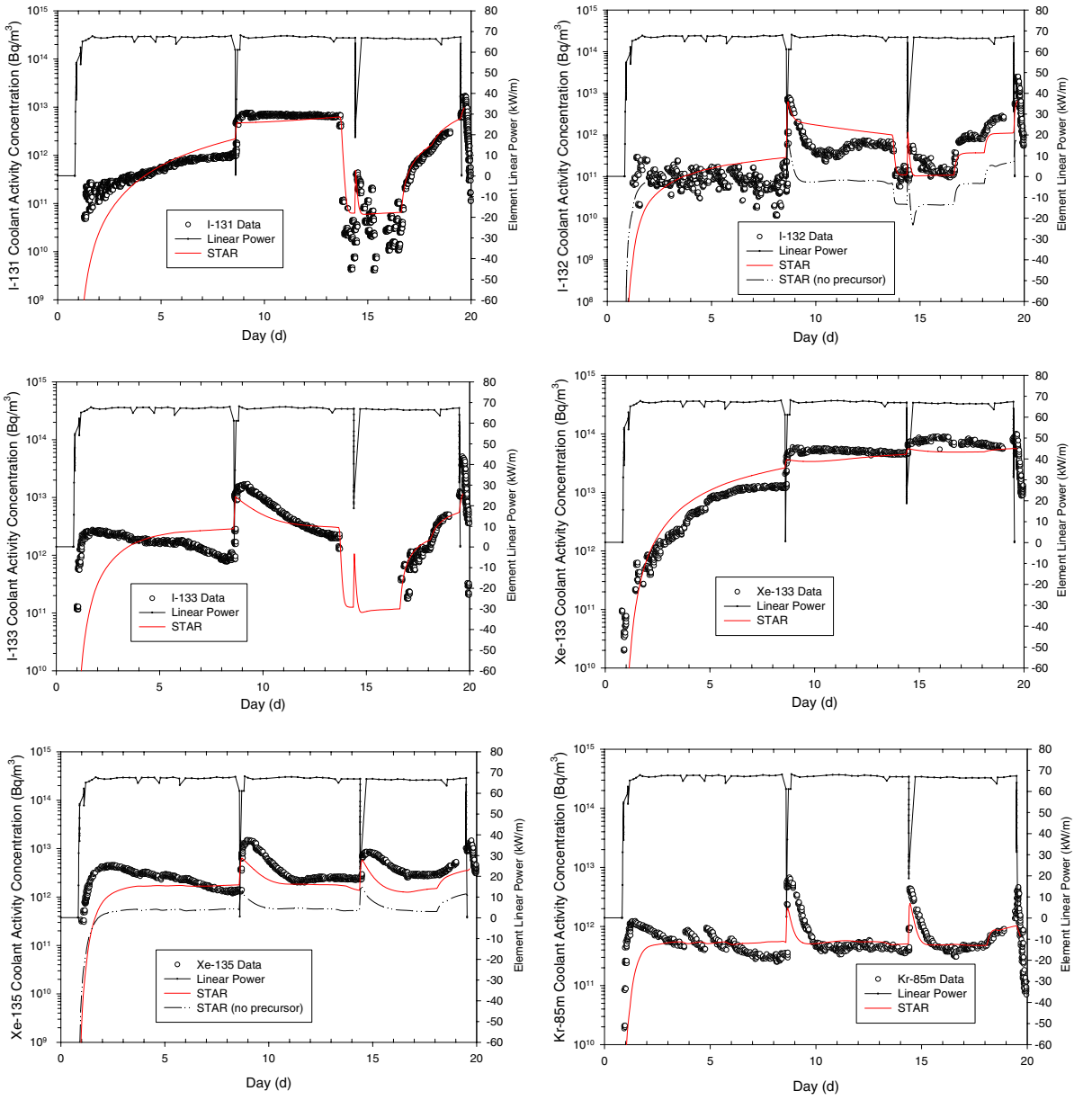

Fig. 7. Comparison between the measured and predicted coolant activity concentration history for iodine and noble gas species for experiment FFO-102-2.

GFP and CEM samples) for the monitored isotopes of ^{131}I and ^{133}Xe with the predicted quantities as shown in Figs. 10 and 11. The model is also able to predict 'iodine-spiking' phenomenon with bundle shifting/reactor shutdown. Spiking of noble gases is further modeled with STAR during transient operation. Interestingly, noble-gas spiking is also observed on shutdown for the commercial defects (i.e., for the horizontal orientation of the CANDU fuel channel), whereas enhanced releases for the noble gases only occurred on shutdown with the vertically-oriented elements in the X-2 defect loop (where presumably noble gases became trapped at the top of the element when liquid water filled the element) [12].

This model can also be utilized in a prognostic fashion with a fitting of the model to coolant activity behaviour (i.e., to characterize the defect state for the given situation), and then predicting the coolant activity for a variable reactor power or

Table 3
Details of selected cases of commercial defect experience as used for STAR validation

Survey case number[a]	Failed fuel identification	Date (position)		Fuel shift dates (position)[b]		Defect description	
		Loading	Discharge	Shift 1	Shift 2	Primary cause	Examination details
1	R04508Z	20 November 99	8 May 00	13 March 00	7 May 00	Incomplete weld	Broken hydride blister (5 mm diameter). Only defect on element
4	XZ2513Z	18 January 03	17 June 03	11 April 03		Debris Fretting	Fully-separated upstream end cap. Small fretted hole in sheath in weld upset (0.1 mm × 0.1 mm)

[a] Case number as given in [37].

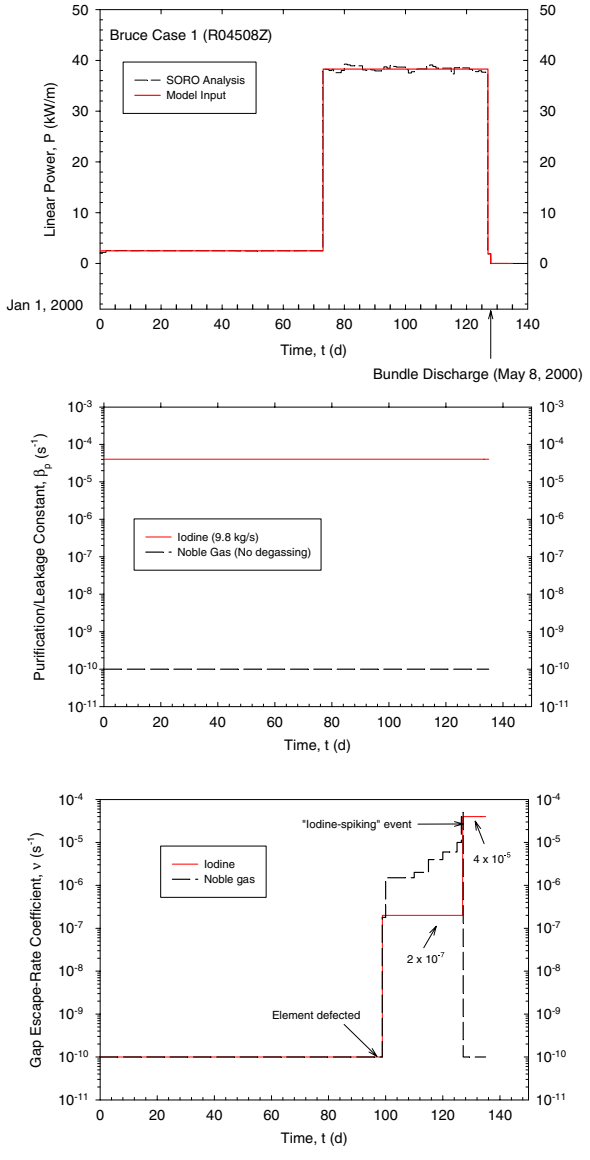

Fig. 8. Input parameters for the simulation of Case 1.

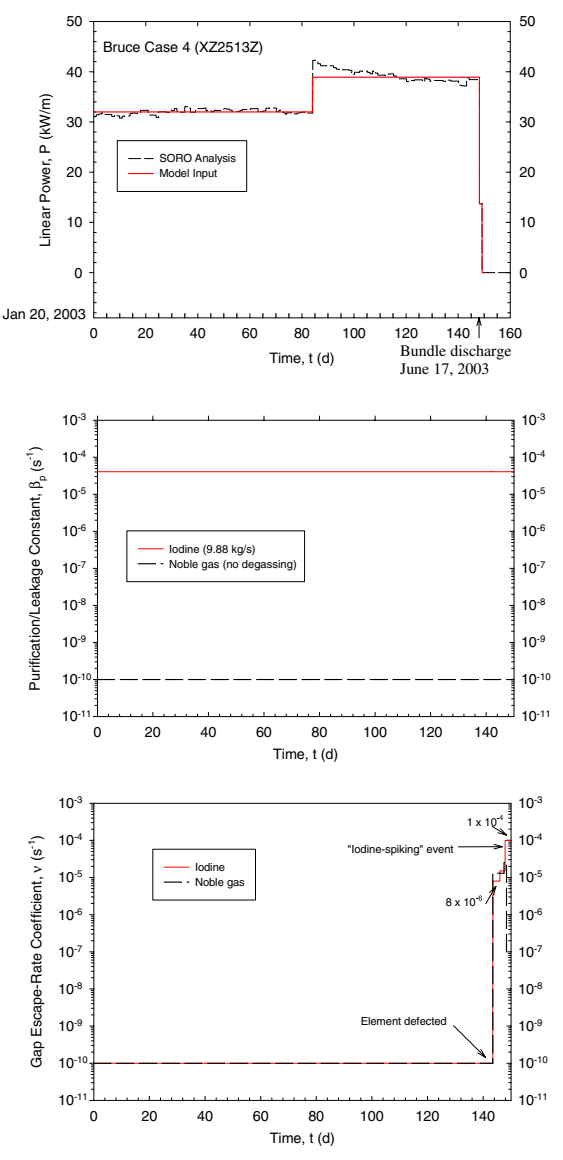

Fig. 9. Input parameters for the simulation of Case 4.

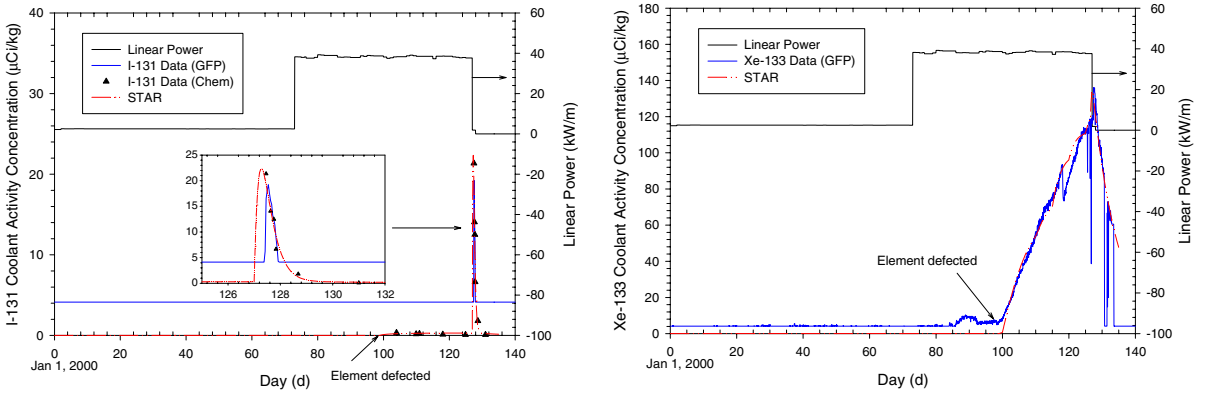

Fig. 10. Comparison between the measured and predicted coolant activity concentration history for iodine and noble gas species for Case 1.

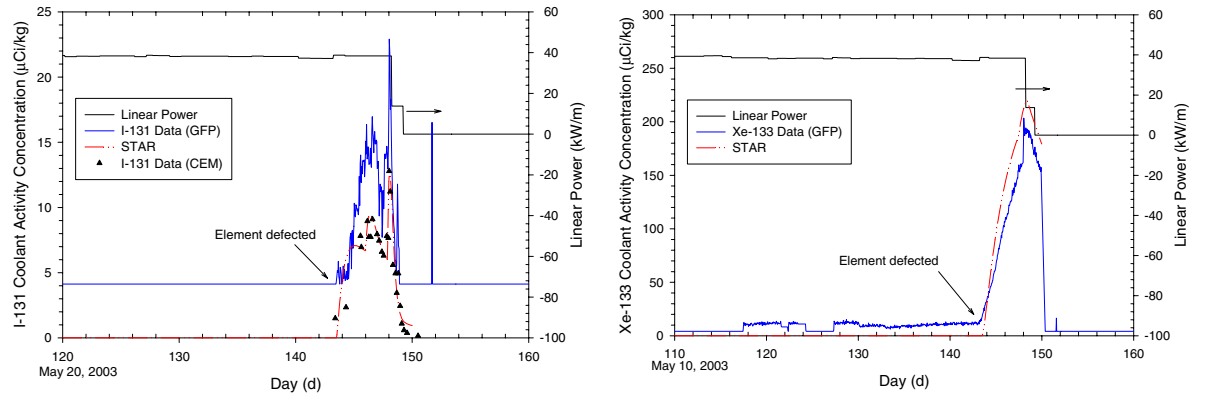

Fig. 11. Comparison between the measured and predicted coolant activity concentration history for iodine and noble gas species for Case 4.

coolant purification history. For instance, the license limit value for the coolant activity concentration of ^{131}I has continually decreased over the years and is quite restrictive. Moreover, once a limit is reached, the operator has 24 h for completion of defect identification/location, defuelling and confirmation activities. With general aging deficiencies of the (on-line) failed defect location system, it may be difficult to locate and remove defective fuel from the core [39]. Thus, with just a few (high-powered) defective elements in-core, a transient iodine spike could force the shutdown of a reactor. Once the reactor is shutdown, failed-bundle localization becomes significantly more difficult since the localization technique is only effective at power [38]. The STAR tool could therefore be useful to estimate if an ^{131}I defect management guideline or license limit would be approached [38,39]. The model could therefore be used to estimate, in a predictive manner, the coolant activity levels that will be reached as steady-state operation is approached or during reactor transient maneuvers given the reactor power and purification flow history. Hence, this work can also help provide an indication of how long the reactor operator has in order to discharge defective fuel before a regulatory limit is reached and how operations may be planned in order to minimize the coolant activity levels [38]. Moreover, similar to the steady-state treatments, a fitting of the more general model to the coolant activity data can also provide diagnostic information on the power of the defective rod(s) (i.e., from the value of the empirical diffusion coefficient assuming Eq. (14) for a 'typical' commercial type failure) as well as the defect state (i.e., from the value of the gap escape-rate coefficient in comparison to that obtained for the well-characterized X-2 defect experiments in Tables 1 and 2) [38].

4. Conclusions

1. A general time-dependent model entitled STAR (Steady-state and Transient Activity Release) has been developed to detail the coolant activity

behaviour of the short-lived iodine and noble gas species during steady reactor operation, as well as for transient conditions of reactor shutdown, startup and bundle-shifting operations. The fission product transport model is based on solid-state diffusion in the fuel matrix and first-order kinetics in the fuel-to-sheath gap. The effect of precursor diffusion and neutron absorption has been incorporated into the treatment. The loss of fission products by radioactive decay and coolant purification (i.e., ion exchange and degassing operations) has also been considered. This model has been solved numerically using the FEMLAB finite-element solver. The model can be used for prediction of the activity in both the fuel-to-clad gap and primary coolant for defective fuel as a function of time.

2. The code has been tested against an analytical solution of the coolant activity. The model has been benchmarked against well-characterized in-reactor experiments with defective elements conducted in the X-2 defect loop facility at the CRL. The fitting parameters of the model are consistent with a previous steady-state analysis. The model has been further validated against several defect occurrences in the commercial NGS (where a single failure was present). The code is successfully able to predict the iodine and noble gas inventory during steady operation as well as enhanced releases in the primary coolant that occur during reactor shutdown, startup and bundle shifting operations.

Acknowledgements

The authors would like to acknowledge the assistance and support of the Reactor Safety Engineering Department and the Nuclear Safety Analysis and Support Department of Bruce Power. The authors also wish to thank M.R. Floyd (CRL) for discussions on defective fuel behaviour. The authors also acknowledge the data made available under the joint Atomic Energy of Canada Limited-Ontario Hydro X-2 Defect Program.

References

[1] B.J. Lewis, C.R. Phillips, M.J. Notley, Nucl. Technol. 73 (1986) 72.
[2] B.J. Lewis, J. Nucl. Mater. 160 (1988) 201.
[3] B.J. Lewis, R.J. Green, C. Che, Nucl. Technol. 98 (1992) 307.
[4] B.J. Lewis, R.D. MacDonald, N.V. Ivanoff, F.C. Iglesias, Nucl. Technol. 103 (1993) 220.
[5] B.J. Lewis, in: Sixth International Conference on CANDU Fuel, Niagara Falls, Ontario, Vol. 1, 26–29 September 1999, p. 403. ISBN 0-919784-62-3.
[6] B.J. Lewis, F.C. Iglesias, D.S. Cox, E. Gheorghiu, Nucl. Technol. 92 (1990) 353.
[7] B.J. Lewis, B. Szpunar, Seminar on Fission Gas Behaviour in Water Reactor Fuels, Cadarache, France, 26–29 September 2000.
[8] B.J. Lewis, D.B. Duncan, C.R. Phillips, Nucl. Technol. 77 (1987) 303.
[9] B.J. Lewis, in: Proceedings of the Third International Conference on CANDU Fuel, Chalk River, Canada, 4–6 October 1992, p. 6–11. ISBN 0-919784-25-9.
[10] B.J. Lewis, F.C. Iglesias, A.K. Postma, D.A. Steininger, J. Nucl. Mater. 244 (1997) 153.
[11] W.N. Bishop, Iodine spiking, EPRI NP-4595, Electric Power Research Institute, 1986.
[12] B.J. Lewis, R.D. MacDonald, H.W. Bonin, Nucl. Technol. 92 (1990) 315.
[13] B.J. Lewis, J. Nucl. Mater. 148 (1987) 28.
[14] B.J. Lewis, B. Szpunar, F.C. Iglesias, J. Nucl. Mater. 306 (2002) 30.
[15] W.T. Thompson, B.J. Lewis, F. Akbari, D.M. Thompson, in: Proceedings of the Eighth International Conference on CANDU Fuel, Honey Harbour, Ontario, 21–24 September 2003.
[16] B.J. Lewis, W.T. Thompson, F. Akbari, C. Thurgood, in: Proceedings of the Eighth International Conference on CANDU Fuel, Honey Harbour, Ontario, 21–24 September 2003.
[17] B.J. Lewis, W.T. Thompson, F. Akbari, D.M. Thompson, C. Thurgood, J. Higgs, J. Nucl. Mater. 328 (2004) 180.
[18] R. Beraha, G. Beuken, G. Frejaville, C. Leuthrot, Y. Musante, Nucl. Technol. 49 (1980) 426.
[19] D.L. Burman, O.A. Correal, H.W. Wilson, H. Kunishi, L.H. Boman, in: Proceedings of the International Top. Mtg. LWR Fuel Performance, Avignon, France, 21–24 April 1991, p. 363, American Nuclear Society, 1991.
[20] C.E. Beyer, Methodology estimating number of failed fuel rods and defect size, EPRI NP-6554, Electric Power Research Institute, 1989, September.
[21] A.H. Booth, A suggested method for calculating the diffusion of radioactive rare gas fission products from UO_2 fuel elements and a discussion of proposed in-reactor experiments that may be used to test its validity, AECL-700, Atomic Energy of Canada Limited, 1957.
[22] G.V. Kidson, J. Nucl. Mater. 88 (1980) 299.
[23] S.D. Beck, The diffusion of radioactive fission products from porous fuel elements, USAEC Report BMI – 1433, 12 April 960.
[24] J.C. Killeen, J.A. Turnbull, in: Proceedings of the Workshop Chemical Reactivity of Oxide Fuel and Fission Product Release, Gloucestershire, England, 7–9 April 1987, p. 387, Central Electricity Generating Board, 1987.
[25] C. Wise, J. Nucl. Mater. 136 (1985) 30.
[26] G.M. Allison, R.F.J. Robertson, The behaviour of fission products in pressurized-water systems (A Review of Defect Tests on UO_2 Fuel Elements at Chalk River), Atomic Energy of Canada Limited report AECL-1338, September 1961.

[27] FEMLAB User's Guide, COMSOL AB, Burlington, MA, USA, 2004.
[28] B.J. Lewis, A. Husain, J. Nucl. Mater. 312 (2003) 81.
[29] R.L. da Silva, Irradiation of a CANDU UO_2 fuel element with twenty-three machined slits cut through the zircaloy sheath, Atomic Energy of Canada Limited report, AECL-8260, September 1984.
[30] R.L. da Silva, N. Macici, The irradiation performance of a naturally defective CANDU UO_2 fuel element power cycled between linear powers of 25–14 kW/m and 38–22 kW/m in the X-2 loop of NRX, Chalk River Nuclear Laboratories report CRNL-2674, September 1984.
[31] M.R. Floyd, Behaviour of a zircaloy-sheathed UO_2 fuel element containing an end cap porosity defect irradiated in the X-1 and X-2 loops at an average linear heat output of 23 kW/m, Chalk River Nuclear Laboratories report CRNL-2687, July 1984.
[32] B.J. Lewis, Behaviour of a zircaloy-sheathed UO_2 fuel element containing a porous end plug defect and exhibiting secondary sheath hydriding irradiated in pressurized light water at a linear power of 67 kW/m, Chalk River Nuclear Laboratories report CRNL-2473, May 1983.
[33] R.L. Da Silva, D.R. McCracken, K.J. Monserrat, in: I.J. Hastings (Ed.), Advances in Ceramics, Fission-Product Behaviour in Ceramic Oxide Fuel, vol. 17, American Ceramic Society, Columbus, Ohio, 1986, p. 107.
[34] B.J. Lewis, Visual_DETECT: A Software Package For Fuel-Failure Monitoring For GFP/Grab Sampling Analysis, Volume 1: Theory Manual, Bruce Power report, December 2003.
[35] C.E.L. Hunt, B.J. Lewis, in: Proceedings of the Fourth International Conference on CANDU Fuel, Pembroke, Ontario, 1–4 October 1995, p. 4B1-14. ISBN 0-919784-52-6.
[36] E. Schuster, F. Garzarolli, A. Kersting, K.H. Neeb, H. Stehle, Nucl. Eng. Des. 64 (1981) 81.
[37] R. Oduntan, F. Iglesias, R. Stone, J. Armstrong, B. Lewis, in: Proceedings of the Ninth International Conference on CANDU Fuel, Belleville, Ontario, 18–21 September 2005.
[38] R. Oduntan, F. Iglesias, R. Stone, J. Armstrong, B. Lewis, in: Proceedings of the Ninth International Conference on CANDU Fuel, Belleville, Ontario, 18–21 September 2005.
[39] R. Stone, J. Armstrong, F. Iglesias, R. Oduntan, B. Lewis, in: Proceedings of the Ninth International Conference on CANDU Fuel, Belleville, Ontario, 18–21 September 2005.